

NEW COREFLOOD INTERPRETATION METHOD BASED ON DIRECT PROCESSING OF IN-SITU SATURATION DATA

Matthew Goodfield, Stephen G Goodyear and Peter H Townsley

AEA Technology plc
Winfrith, Dorchester, Dorset, DT2 8ZE, United Kingdom

Abstract

Generation of good quality relative permeability data depends on carefully designed programmes of core flooding, combined with appropriate interpretation of the basic laboratory data. Where capillary pressure is important, the JBN technique can give misleading results. In this case, simulation methods can be used to model the influence of capillary pressure. However, experience shows that the conventional fixed capillary pressure outlet boundary condition may fail to capture the development of the in-situ saturation profiles satisfactorily.

This paper describes a new approach to coreflood interpretation, which fully utilises in-situ saturation data and reduces the sensitivity to assumptions about the core boundary conditions. The new method extends previously published techniques for the interpretation of gravity drainage floods by including viscous and capillary forces. Relative permeabilities are calculated directly from in-situ saturation and pressure drop data, without the need to use simulation methods, by applying the Darcy flow equations for the mobile phases at each position and time in the core. Darcy's equations are recast to give separate pressure and fractional flow equations. The fractional flow equation is solved locally, independently of any boundary condition assumptions, and the pressure equation (written in a global integral form) is solved for the mobility. The algorithm is applicable to a wide range of water-oil displacements or gas-oil displacements with an immobile initial water saturation, including multi-rate and constant pressure drop unsteady-state floods, steady-state and gravity drainage floods.

Synthetic saturation and pressure drop data sets have been generated using a conventional simulator for a selection of water/oil and gas/oil core floods. The algorithm is applied to the data sets to construct the underlying relative permeabilities, including a significant fraction of the oil relative permeability tail. The presence of capillary end effects allows relative permeabilities at some saturations below the Buckley-Leverett shock front to be calculated in unsteady-state displacements. A range of smoothing methods have been developed to allow the basic algorithm to be successfully applied to datasets in which noise has been added to the basic saturation and pressure profiles generated by simulation.

Introduction

Laboratory special core analysis (SCAL) water or gas flooding studies to determine relative permeabilities need to be performed in such a way that they are representative of reservoir conditions. The importance of preparation methods to condition the core to an appropriate initial water saturation and wettability, together with the choice of fluids and flooding rates, are increasingly recognised as key elements of definitive SCAL programmes.

The results from core floods need to be interpreted to determine relative permeabilities. For example, the conventional Johnson Bossler and Naumann (JBN) interpretation method [1] uses oil production and pressure drop data to calculate relative permeabilities, assuming that the influence of capillary pressure on the displacement can be neglected. However, where capillary pressure is important, (Figure 1), the JBN method can give misleading results, overestimating the residual oil saturation and giving artificially suppressed relative permeabilities. The influence of capillary pressure can be reduced by increasing the displacement rate. However, high flow rates can change the character of the displacement, especially at intermediate-wet conditions, making results unrepresentative of the reservoir.

In-situ saturation monitoring is a powerful tool for identifying displacements influenced by capillary pressure. Where capillary pressure is shown to be important more sophisticated interpretation methods are required, if meaningful relative permeabilities are to be calculated. Current best practice uses simulation

methods to include the influence of capillary pressure. Separately measured static capillary pressure and/or limited in-situ saturation data are used to constrain regression methods to fit to production and pressure drop data [2-5]. This approach is an indirect method, using a series of simulations combined with information about the goodness of fit to the chosen data to adjust the choice of relative permeabilities and capillary pressure. Where an independent measurement of capillary pressure is made on a second core, it may be difficult to ensure that it is representative of the original reservoir rate displacement test. The regression problem is made difficult by the large number of strongly coupled parameters that characterise the relative permeabilities and capillary pressure. Experience shows that the results often fail to capture the development of in-situ saturation data satisfactorily, especially at the core outlet where a fixed saturation (corresponding to the conventional zero capillary pressure boundary condition) may not be observed.

Good quality in-situ saturation data is often measured during SCAL studies. A number of methods have been developed to make use of this data, for example in [6] relative permeabilities are calculated for saturations on the displacement front. An alternative approach to interpreting in-situ data has been applied to gravity drainage core floods, which allows relative permeabilities to be deduced directly from in-situ saturation data. This uses the change in saturation profiles with time to calculate the local phase Darcy velocity, which can then be related directly to relative permeability in regions of the core where capillary forces are small compared to gravity forces. The method has been successfully applied in a number of studies of gravity drainage [7-9]. This work builds on these ideas by fully accounting for the influence of viscous and capillary forces, in addition to gravity forces.

Formulation of basic equations

It is assumed that the core can be treated as a homogeneous one dimensional system. The basic equations are used to describe water/oil displacements or gas/oil displacements with a uniform immobile initial water saturation. In this paper the equations are derived in notation appropriate for a vertical water/oil displacement, but they can easily be translated to horizontal cores (by setting $g = 0$) or gas/oil displacements. Distance along the core is measured from the inlet, which is assumed to be at the base of the core.

The starting point for the new interpretation methods is Darcy's law, where the phase velocities are expressed according to:

$$U_a = -kI_a \left(\frac{\int p_a}{\int z} + r_a g \right) \quad (1)$$

where I_w and I_o are the water and oil phase mobilities respectively, defined by:

$$I_a = k_{ra} / m_a \quad (2)$$

and the water/oil capillary pressure $p_{cw}(S_w)$ is defined in the standard convention by:

$$p_{cw}(S_w) = p_o(S_w) - p_w(S_w). \quad (3)$$

Coreflooding sequences are normally designed so that any change in the fluid volumes due to the pressure drop along the core can be neglected so that the total Darcy velocity $U(t)$ is known. This allows the Darcy equation for each phase to be re-cast to separate the pressure and fractional flow terms.

Saturation equation

The pressure independent equation forms an extension of the familiar fractional flow equation:

$$U_o = U(t) \frac{I_o}{I_w + I_o} \left(1 + \frac{kg(r_w - r_o)}{U(t)} I_w \right) - k \frac{I_o I_w}{I_w + I_o} \frac{dp_{cw}}{dS_w} \frac{\int S_w}{\int z}. \quad (4)$$

This comprises a convective and dispersive term which can be summarised as:

$$U_o = U(t) f_o^{(g)}(S_w, U) + kd_{cpw}(S_w) \frac{\int S_w}{\int z}, \quad (5)$$

where the gravity fractional flow $f_o^{(g)}$ is given by

$$f_o^{(g)}(S_w, U) = f_o(S_w) + \frac{k}{U} G_o(S_w), \quad (6)$$

f_o is the conventional viscous dominated fractional flow curve:

$$f_o(S_w) = \frac{I_o}{I_w + I_o}, \quad (7)$$

and G_o is the gravity counter-current flow velocity function defined by

$$G_o(S_w) = g(\mathbf{r}_w - \mathbf{r}_o) \frac{I_o I_w}{I_w + I_o}, \quad (8)$$

In the absence of gravity the gravity fractional flow $f_o^{(g)}$ reduces to the conventional viscous dominated fractional flow curve f_o . The capillary dispersion rate function d_{cpw} is given by

$$d_{cpw}(S_w) = -\frac{I_o I_w}{I_w + I_o} \frac{dp_{cw}}{dS_w} \quad (9)$$

and corresponds to the counter-current flow term associated with capillary imbibition.

This construction of the oil Darcy velocity equation in terms of $f_o^{(g)}$ and d_{cpw} represents a “natural parameterisation” of the equation with the separate terms having a clear physical meaning. Where gravity can be neglected compared to viscous and capillary forces, or where flow is at a constant total rate, the evolution of saturations within the core is controlled explicitly just by these two independent functions. This contrasts with the conventional approach where three separate functions are considered (two relative permeabilities and a capillary pressure) even when handling just the saturation data.

Pressure equation

Since pressure data is usually known at a few points, often only at the ends of the core, a more global form of the pressure equation has to be formulated to make use of this information. One of the difficulties encountered here is a possible ambiguity in how pressures measured in the inlet and outlet lines are related to phase pressures in the core at the inlet and outlet face (since the oil and water phase pressures are different by the capillary pressure).

It is reasonable to assume that the inlet pressure corresponds to the water phase pressure at the inlet face of the core (subject to gravity head corrections) and that at some point after water breakthrough the outlet pressure corresponds to the water phase pressure at the outlet face of the core. In this case the pressure difference can be determined by re-arranging and integrating Equation 1 along the length of the core:

$$\Delta p(t) = g \mathbf{r}_w L + \int_0^L \frac{U_w(z, t)}{k I_w(S(z, t))} dz. \quad (10)$$

Prior to water breakthrough the outlet pressure will correspond to the oil phase pressure at the outlet face of the core. The pressure drop can then be expressed in the following form:

$$\begin{aligned} \Delta p(t) = & g \mathbf{r}_w z^{(p)}(t) + g \mathbf{r}_o (L - z^{(p)}(t)) \\ & - p_{cw}(S_w^{(p)}) + \int_0^{z^{(p)}(t)} \frac{U_w(z, t)}{k I_w(S(z, t))} dz + \int_{z^{(p)}(t)}^L \frac{U_o(z, t)}{k I_o(S(z, t))} dz \end{aligned} \quad (11)$$

where $z^{(p)}(t)$ is the position of a fixed saturation $S_w^{(p)}$ at time t (known from the saturation data). These equations may also be expressed in terms of the total mobility and the gravity fractional flow instead of the phase mobilities.

Solution of equations

The *dyrectSCAL* (*d*ynamic *r*elative permeability - *c*apillary pressure *t*echnique *S*CAL) algorithms handle the saturation and pressure data separately. Using information about local phase Darcy velocities and saturation gradients, the gravity fractional flow curve and capillary dispersion rate function are constructed to satisfy equation 5. The pressure equation is then solved for the water mobility. Finally, the relative permeabilities and capillary pressure are deconvoluted from the results of the analysis of the saturation and pressure equation. This section describes these stages in detail for the algorithms applied to saturation data

defined continuously in space and time. For processing actual data, discrete representations of the algorithms are needed, with the requirement for appropriate data smoothing and interpolation techniques.

Local phase Darcy velocity

Analysis of equation 5 requires that the local Darcy phase velocities are known. These may be calculated from the in-situ saturations and the injection history using a material balance approach:

$$U_o(z, t) = U(t)F_o^{inj}(t) - \frac{\int V_o(z, t)}{\int t}, \quad (12)$$

where the phase volumes per unit cross-sectional area between the core inlet and position z are given by

$$V_o(z, t) = \int_0^z f(z)S_o(z, t)dz \quad (13)$$

and $F_o^{inj}(t)$ is the fractional flow of oil injected at time t .

Direct solution of saturation equation

Direct solution of the saturation equation 5 is made at a series of fixed saturations. For a given saturation S_w^* the corresponding positions for this saturation in the core as a function of time, are evaluated according to:

$$S_w(z^*(t), t) = S_w^* \quad (14)$$

thereby determining the trajectory of the saturation S_w^* in z - t space. Rewriting equation 5 in terms of z^* and t gives the following form:

$$U_o(z^*, t) = U(t)f_o^{(g)}(S_w^*, U) + kd_{cpw}(S_w^*) \frac{\int S_w}{\int z} \Big|_{z^*, t} \quad (15)$$

Except in the special case of zero total Darcy velocity (considered below), equation 15 can be rearranged to give:

$$\frac{U_o(z^*, t)}{U(t)} = f_o^{(g)}(S_w^*, U) + d_{cpw}(S_w^*) \frac{k}{U(t)} \frac{\int S_w}{\int z} \Big|_{z^*, t} \quad (16)$$

where $U_o(z^*, t)$ and $\frac{\int S_w}{\int z} \Big|_{z^*, t}$ are calculated from the observed saturation data. Provided gravity forces are

negligible, or for periods of time when the total flowrate is constant, this equation gives $\frac{U_o(z^*, t)}{U(t)}$ as a linear

function of $\frac{k}{U(t)} \frac{\int S_w}{\int z} \Big|_{z^*, t}$, where the intercept is given by $f_o^{(g)}(S_w^*, U)$ and the gradient by $d_{cpw}(S_w^*)$. Thus

plotting the observed values of $\frac{U_o(z^*, t)}{U(t)}$ against $\frac{k}{U(t)} \frac{\int S_w}{\int z} \Big|_{z^*, t}$, and performing a linear regression allows

$f_o^{(g)}(S_w^*, U)$ and $d_{cpw}(S_w^*)$ to be evaluated.

Figure 2 shows this process schematically. In the case of no capillary pressure, a line of zero slope will be found, corresponding to the conventional Buckley-Leverett solution. Where capillary pressure is important, a line with non-zero slope will be found. It is also worth noting the possibility of not being able to separate out information about $f_o^{(g)}(S_w^*, U)$ and $d_{cpw}(S_w^*)$ in the special case of the saturation corresponding to one on a stabilised front, where all the data would group around a single point. However, to what extent this would actually arise in practice is open to question, since data early in the flood may be too early for the stabilised front to have been established, and in regions at the end of the core influenced by capillary end effects the stabilised zone may be disrupted.

Repeating this procedure for different values of S_w^* allows the gravity fractional flow and capillary dispersion function to be constructed. A number of important features of this algorithm are worth noting:

- the most important reservoir engineering function, $f_o^{(g)}$, determining the local sweep efficiency of a water flood is obtained
- the calculation of $f_o^{(g)}$ and d_{cpw} is purely local, and no assumptions about the inlet and outlet boundary conditions are required
- $f_o^{(g)}$ and d_{cpw} are constructed explicitly on a pointwise basis, so that no particular functional forms need to be assumed
- the method can be applied to data irrespective of the type of flooding procedure used, i.e. multi-rate tests, unsteady-state tests, steady-state tests and gravity drainage (subject to the assumption of a non-zero total Darcy velocity and either negligible gravity forces or periods of constant total flow rate)
- where a composite core is used, the regression can be applied to each plug separately, allowing $f_o^{(g)}$ and d_{cpw} to be evaluated for each plug
- the method can be applied to the dynamic data between established steady-state conditions (the special case of analysis of the steady-state data is discussed below)
- the constructional nature of the algorithm demonstrates that an independent measurement of capillary pressure is not required to interpret insitu saturation data in the presence of capillary end effects.

Pure counter-current flow and gravity dominated solution

In the case of pure counter-current flow the total Darcy velocity is zero and the formulation of the basic saturation equation is made in terms of G_o and d_{cpw} according to:

$$\frac{U_o(z^*, t)}{k} = G_o(S_w^*) + d_{cpw}(S_w^*) \left. \frac{\mathcal{I}S_w}{\mathcal{I}z} \right|_{z^*, t} \quad (17)$$

The gravity dominated ($U \ll kI_w g(\mathbf{r}_w - \mathbf{r}_o)$) version of the saturation equation also takes this form.

Plotting $\frac{U_o(z^*, t)}{k}$ against $\left. \frac{\mathcal{I}S_w}{\mathcal{I}z} \right|_{z^*, t}$ and performing a linear regression allows $G_o(S_w^*)$ and $d_{cpw}(S_w^*)$ to be evaluated. Where the solution is gravity dominated and the additional condition that the oil mobility is low compared to the water mobility holds ($I_o \ll I_w$), $G_o(S_w^*)$ reduces to:

$$G_o(S_w^*) \approx g(\mathbf{r}_w - \mathbf{r}_o) I_o(S_w^*) \quad (18)$$

allowing the oil relative permeability to be calculated directly.

Steady-state tests

If only the steady-state conditions are to be analysed, there is no need to calculate local phase Darcy velocities, since these are known from the imposed fractional flow. Equation 16 simplifies to:

$$F_o^{inj}(t) = f_o^{(g)}(S_w^*, U) + d_{cpw}(S_w^*) \frac{k}{U(t)} \left. \frac{\mathcal{I}S_w}{\mathcal{I}z} \right|_{z^*, t} \quad (19)$$

Provided capillary forces are sufficiently important for a given saturation to be present in the core on a number of equilibrium states this equation may be analysed in the standard way, subject to the normal assumptions that gravity forces are negligible or the total flowrate is constant.

Multi-rate tests where gravity is not negligible

In the case where gravity forces are not negligible, and $f_o^{(g)}(S_w^*, U)$ has been deduced from data corresponding to periods of constant flow at a number of total Darcy velocities U_i , it is possible to deduce $f_o(S_w^*)$ and $G_o(S_w^*)$ according to the following analysis:

$$f_o^{(g)}(S_w^*, U_i) = f_o(S_w^*) + \frac{k}{U_i} G_o(S_w^*) \quad (20)$$

Then by plotting $f_o^{(g)}(S_w^*, U_i)$ against k/U_i and performing a linear regression allows $f_o(S_w^*)$ and $G_o(S_w^*)$ to be evaluated. For saturations where this is possible, this determines three independent functions and so allows the relative permeabilities and capillary pressure gradient to be determined without using pressure drop data (avoiding the complications of boundary condition effects). This result is possible because the different flow rates are combined with a known local gravitational pressure gradient.

Gravity and generally varying flow rates

In the case of a generally varying flowrate it is possible to write the saturation equation in the following form:

$$\frac{U_o(z^*, t)}{k} = G_o(S_w^*) + \frac{U(t)}{k} f_o(S_w^*) + d_{cpw}(S_w^*) \frac{\int S_w}{\int z} \Big|_{z^*, t} \quad (21)$$

$\frac{U_o(z^*, t)}{k}$ is then a linear function of $\frac{U(t)}{k}$ and $\frac{\int S_w}{\int z} \Big|_{z^*, t}$, in principle allowing $G_o(S_w^*)$, $f_o(S_w^*)$ and

$d_{cpw}(S_w^*)$ to be determined from a 2-D linear regression. However, for practical cases, insufficient data in

$\frac{U(t)}{k}$ and $\frac{\int S_w}{\int z} \Big|_{z^*, t}$ space may be available to make this generally applicable.

Direct solution of pressure equation

Solution of the pressure equation (equation 10) requires the water mobility to be determined. In practice, pressure drop data is often quite noisy, especially when floods are conducted at reservoir conditions. The solution algorithm is based on a least squares regression on the pressure equation, by varying a parameterised version of the water mobility.

Note that while the fractional flow curve constructed by the methods of the previous section is well defined, the data for the pressure equation and its interpretation is more uncertain. However, this ambiguity will only feed through into the total mobility function and the full capillary pressure curve, which in many cases will make less impact on predictions of reservoir performance.

Construction of relative permeability and capillary pressure

The oil mobility, and hence relative permeabilities, are determined by solving equation 6. The capillary pressure gradient can then be calculated using the known form of d_{cpw} and the mobility functions. The capillary pressure curve is then evaluated to within a constant by integration. The absolute level of the capillary pressure would be known if it proves possible to determine $p_{cw}(S_w^{(p)})$ from the pressure equation regression if equation 11 is used. Alternatively, the saturation at the core outlet after breakthrough would correspond to zero capillary pressure if the conventional capillary pressure boundary condition is assumed.

If phase selective pressure transducers were utilised [10], that allowed a direct dynamic measurement of capillary pressure to be made, it would be possible to construct the relative permeabilities using this information together with $f_o^{(g)}$ and d_{cpw} deduced from the saturation data. In this scenario the total pressure drop data would no longer be required, completely avoiding the ambiguities associated with this measurement.

Smoothing of saturation data

The *direct*SCAL algorithms described in this paper are based on continuum saturation and pressure data. In practice saturation and pressure data is only measured at discrete spatial positions and times, and the data is subject to statistical noise and local fluctuations associated with small scale heterogeneity. Therefore, the algorithms have been recast in a discrete form, and appropriate smoothing techniques developed. Noisy saturation data is first smoothed before being interpreted using the discrete form of the *direct*SCAL algorithms. A number of smoothing methods have been developed, ranging from parametric non-linear least squares fitting to non-parametric constrained spline methods. These methods have been applied to the saturation-position, saturation-time, position-time and saturation-position-time spaces ($S-z$, $S-t$, $z-t$ and $S-z-t$). The smoothing methods used in each case depend on the type of data being analysed and the nature of the displacement process.

Validation of methods

A conventional black-oil reservoir simulator was used to generate synthetic saturation and pressure drop data. Synthetic data has been generated for a number of different test cases including: gas-oil gravity drainage, unsteady-state water-oil, steady-state water-oil and constant pressure drop gas-oil displacements. A gas-oil gravity drainage displacement and an unsteady-state water-oil displacement are described here. In both these cases a conventional zero capillary pressure boundary condition was applied at the outlet.

A total of 40 equally spaced saturation monitoring positions were assumed along the core and saturation measurements were taken at time intervals of 5 minutes or greater. Uncorrelated Gaussian random noise was then added to the synthetic saturation data to represent the effect of measurement error and small-scale heterogeneity.

Unsteady-state water-oil test

In the unsteady-state test, water was injected in a horizontal 10 cm core at a constant rate of 8 ml hr⁻¹. The synthetic saturation profiles with noise are illustrated in Figure 1. This test was interpreted using the general form of the *direct*SCAL method which uses both the saturation and pressure drop data. As a basic validation of the *direct*SCAL approach, the synthetic saturation data before the addition of noise was processed. The interpreted fractional flow curve is shown in Figures 3 and 4, where it can be seen that the entire fractional flow curve is successfully reconstructed for saturations above about 0.5 (corresponding to a water fractional flow of about 0.3). The error bars show the 90% confidence interval obtained from the linear regression. It should be noted that each data point on the *direct*SCAL fractional flow and dispersion rate functions is individually calculated, entirely independently of the other points and the assumptions made about the core inlet and outlet boundary conditions. The presence of a capillary end effect allows fractional flows significantly below the Buckley-Leverett shock front to be calculated. In contrast, the JBN interpretation of the data shows unrepresentatively early water breakthrough and too high a residual oil saturation. The capillary dispersion rate is also successfully reconstructed for saturations above about 0.5 (Figure 5). For the data set including noise, the interpreted oil gravity fractional flow and capillary dispersion rate functions are compared with the originals in Figures 6 to 8. Figure 6 shows a good match to the shock front saturation and that some data are obtained at lower saturations. This figure also shows that the method becomes less reliable on steep sections of the saturation profiles (in this case at saturations less than 0.55). The log-plot of the fractional flow (Figure 7) shows that low values of the fractional flow can still be recovered.

The relative permeability functions are shown in Figures 9 and 10. Since the water relative permeability was modelled by a parametric form, a smooth curve is obtained. The oil relative permeability is evaluated as a function of the fractional flow and so breaks down at the same point as the fractional flow curve. The water-oil capillary pressure function is shown in Figure 11. The saturation at the outlet has been used to define the zero point on the capillary pressure function. The oil recovery factor is plotted against pore volumes of water injected in Figure 12. There is a very good match for up to two PV injected and a good match above this. This should be contrasted with the basic core flood recovery factor which is lower due to the hold up of oil in

the core by capillary pressure. If a bump flood were incorporated in the test sequence, additional data at the high water saturations would be available for processing, which would be expected to further improve the match to the underlying recovery curve (based on the viscous dominated fractional flow curve). In contrast, the JBN method fails to match the recovery factor in this case.

Gas-oil gravity drainage test

In the gravity drainage test, gas was injected at the top of the vertically oriented 60 cm core at a constant rate of 2 ml hr^{-1} . The synthetic saturation profiles with noise are illustrated in Figure 13. This test was interpreted using the gravity dominated form of the *dyrectSCAL* method which does not use the pressure drop data.

Application of the gravity drainage version of the *dyrectSCAL* algorithm allows the oil relative permeability to be recovered, even from data in regions of the core strongly influenced by capillary pressure. As a basic validation of the *dyrectSCAL* approach, the synthetic saturation data before the addition of noise was processed. The interpreted oil gravity counter-current flow velocity is compared with the original function in Figure 14. This figure shows that the function is successfully reconstructed for saturations above about 0.3. For the data set including noise, the interpreted capillary dispersion rate function is compared with the original function in Figure 15. The corresponding oil relative permeability curves are shown in Figures 16 and 17. At low saturations the gas mobility will become low enough for the displacement to cease to be gravity dominated and the gravity dominated solution will no longer be valid. In this case, the accuracy of the results reduces (with increasing saturation gradient) before this point is reached.

A good match is obtained to the capillary pressure function (Figure 18). This is because only the ratio of the counter-current flow velocity to the dispersion rate is required in the evaluation of the capillary pressure function and it can be shown that this ratio is generally less sensitive to the accuracy of the linear regression for gravity dominated displacements.

Conclusions

1. The equations for coreflood simulation have been reformulated in terms of a “natural parameterisation” of the multi-phase functions each with a clear physical meaning.
2. The evolution of the insitu saturations is determined by only two independent functions, the fractional flow and capillary dispersion function.
3. The in-situ saturation data can be processed using an explicit constructional method (*dyrectSCAL*) to determine the fractional flow and capillary dispersion function, independently of boundary condition assumptions.
4. The explicit construction demonstrates that independent measurements of capillary pressure are not required to interpret core flood data.
5. The pressure equation is solved using local Darcy velocity data without the need for conventional simulation.
6. The *dyrectSCAL* methodology is applicable to a wide range of core flooding methods including unsteady-state, steady-state and gravity drainage floods.
7. The methods have been successfully applied to synthetic data sets, which include noise, by the development of a range of smoothing techniques.

Acknowledgements

AEA Technology is grateful for the financial support for this project from BP Amoco, Shell Expro and the UK Department of Trade and Industry.

Nomenclature

| | | | |
|----------------|---|--------------|--|
| d_{cpw} | capillary dispersion rate [s^{-1}] | t | time [s] |
| f_o | viscous dominated fractional flow [dimensionless] | $U(t)$ | total Darcy velocity [$m\ s^{-1}$] |
| $f_o^{(g)}$ | gravity fractional flow [dimensionless] | U_a | Darcy velocity of phase a [$m\ s^{-1}$] |
| $F_o^{inj}(t)$ | injected fractional flow of oil [dimensionless] | $V_o(z,t)$ | oil volume per unit area in core between inlet and position z [m] |
| g | gravity constant [ms^{-2}] | $z^*(t)$ | distance from inlet of S_w^* at time t [m] |
| G_o | gravity flow function [$m^{-1}s^{-1}$] | $z^{(p)}(t)$ | distance from core inlet of $S_w^{(p)}$ at time t [m] |
| k | permeability [m^2] | z | distance from core inlet [m] |
| k_{ra} | relative permeability of phase a [dimensionless] | Greek: | |
| L | length of core [m] | Δp | core pressure drop [Pa] |
| p_{cw} | water/oil capillary pressure [Pa] | $f(z)$ | porosity [dimensionless] |
| p_a | pressure of phase a [Pa] | l_a | mobility of phase a [$Pa^{-1}s^{-1}$] |
| $S_a(z,t)$ | saturation of phase a [dimensionless] | m_a | viscosity of phase a [Pa s] |
| S_w^* | fixed water saturation used for <i>direct</i> SCAL algorithm [dimensionless] | r_a | density of phase a [$kg\ m^{-3}$] |
| $S_w^{(p)}$ | fixed water saturation used for pre- breakthrough pressure equation [dimensionless] | z | integration variable [m] |
| | | Subscripts: | |
| | | a | phase label |
| | | <i>g</i> | gas phase |
| | | <i>o</i> | oil phase |
| | | <i>w</i> | water phase |

References

- Johnson, E.F., Bossler D.P. and Naumann, V.O., "Calculation of Relative Permeability from Displacement Experiments", *Trans., AIME* (1959), 370-72.
- Richmond, P.C. and Watson, A.T., "Estimation of Multiphase Flow Functions from Displacement Experiments", *SPE Reservoir Engineering*, Feb 1990, 121-27.
- Chardaire-Riviere, C., Jaffre, J. and Liu J., "Multiscale Representation for Simultaneous Estimation of Relative Permeabilities and Capillary Pressure", SPE 20501, presented at 65th Annual Technical Conference, New Orleans, LA, 23-26 September, 1990.
- Chardaire-Riviere, C., Chavent, G., Jaffre, J. and Liu J. and Bourbiaux, B.J., "Simultaneous Estimation of Relative Permeabilities and Capillary Pressure", *SPE Formation Evaluation*, (Dec 1992), pp283-289.
- Mejia, G.M., Mohanty K.K., and Watson, A.T., "Use of In-Situ Saturation Data in Estimation of Two-Phase Flow Functions in Porous Media", *Journal of Petroleum Science and Engineering* (1995) **12** pp233-245.
- Helset H.M., Nordtvedt J.E., Skjaeveland S.M. and Virnovsky G.A., "Relative Permeabilities from Displacement Experiments with Full Account for Capillary Pressure", *SPE Reservoir Evaluation & Engineering*, April 1998, pp92-98 (SPE 36684).
- Foulser, R.W.S., Naylor, P. and Seale, C., "Relative Permeabilities for Gravity Stabilised Gas Injection", *Trans IChemE*, July 1990, **68**, Part A.
- Goodyear, S.G. and Jones, P.I.R., "Relative Permeabilities for Gravity Stabilised Gas Injection", 7th European Symposium on Improved Oil Recovery, Moscow, Russia, October 1993.
- Naylor, P., Sargent, N.C., Crossbie, A.J. and Goodyear, S.G., "Gravity Drainage During Gas Injection", 8th European Symposium on Improved Oil Recovery, Vienna, Austria, 15-17 May 1995.
- van Wunnik, J.N.M., Oedai, S, and Masalmeh, S., "Capillary Pressure Probe for SCAL Applications", SCA-9908, 1999 Society of Core Analysts International Symposium, Golden, 1-4 August.

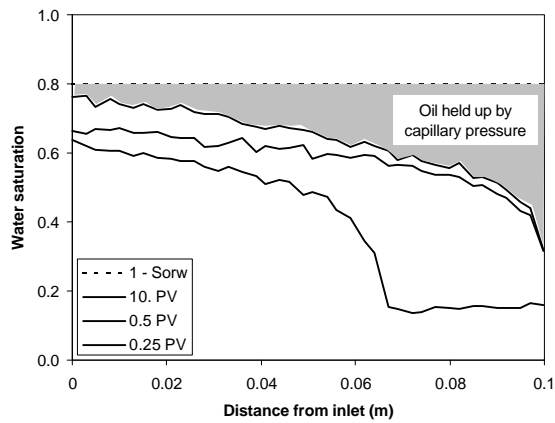


Figure 1 Synthetic water saturations for unsteady state test

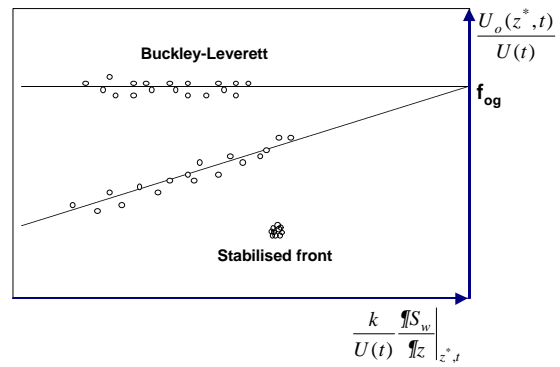


Figure 2 Schematic of direct solution of saturation equations using the *dyrectSCAL* method

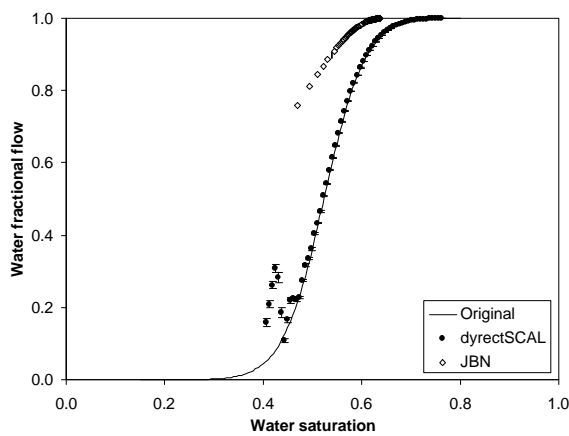


Figure 3 Comparison of interpreted water fractional flow for unsteady state test without noise

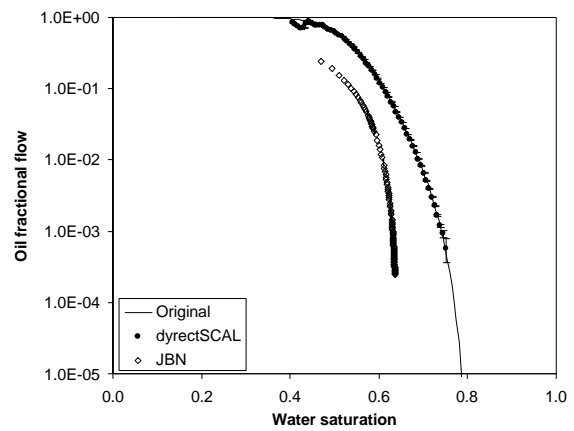


Figure 4 Comparison of interpreted oil fractional flow for unsteady state test without noise

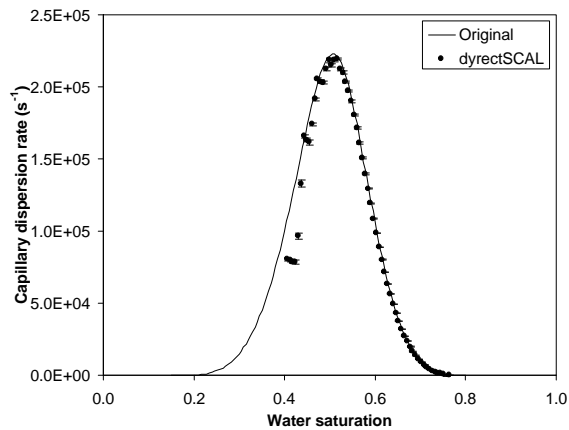


Figure 5 Interpreted capillary dispersion rate for unsteady state test without noise

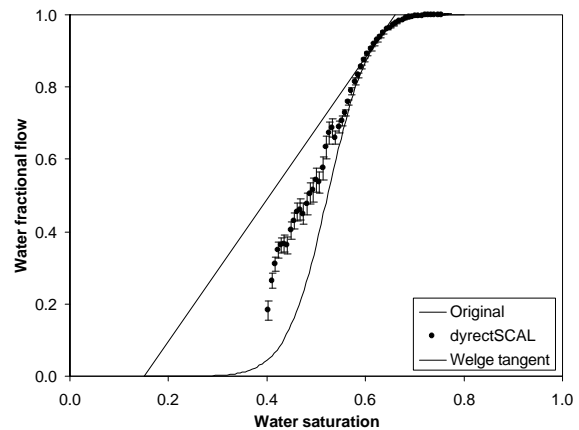


Figure 6 Interpreted water fractional flow for unsteady state test

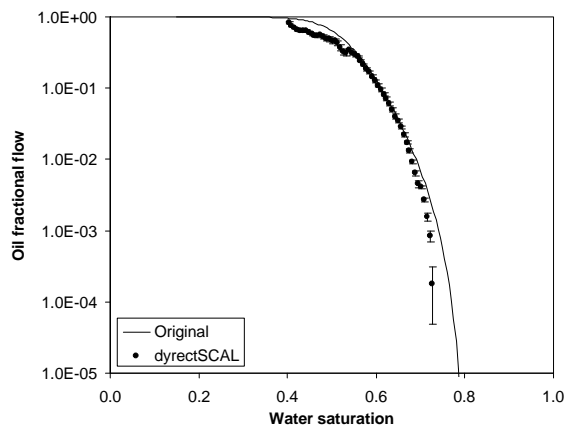


Figure 7 Interpreted oil fractional flow for unsteady state test

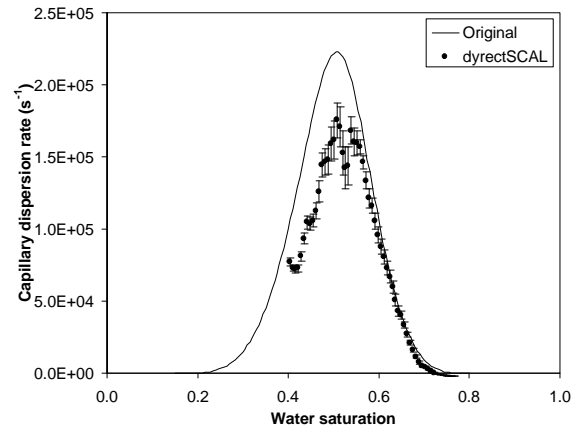


Figure 8 Interpreted capillary dispersion rate for unsteady state test

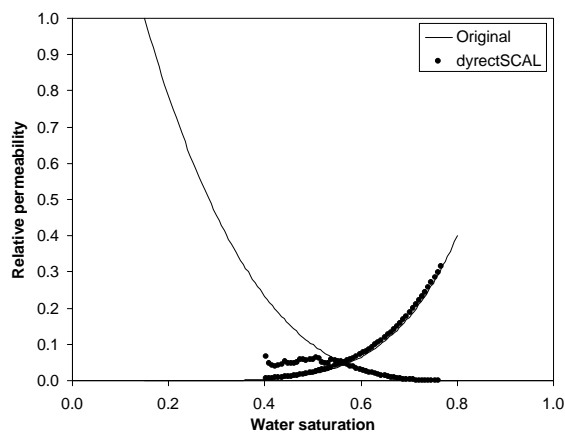


Figure 9 Interpreted oil and water relative permeabilities for unsteady state test

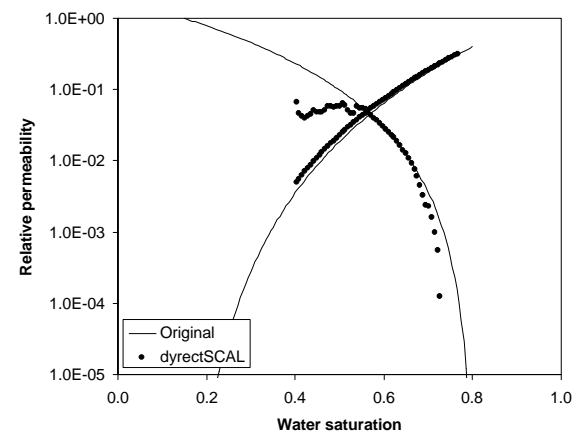


Figure 10 Interpreted oil and water relative permeabilities for unsteady state test

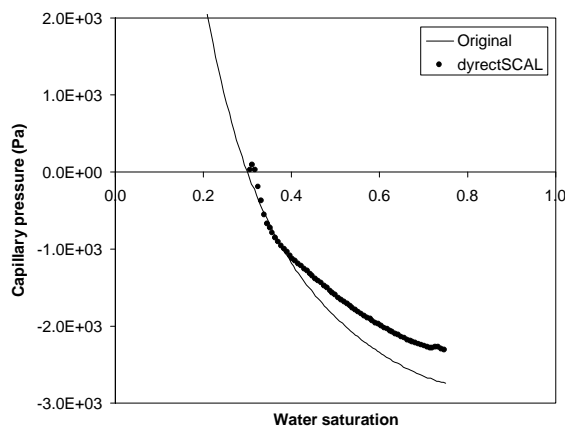


Figure 11 Interpreted water-oil capillary pressure for unsteady state test

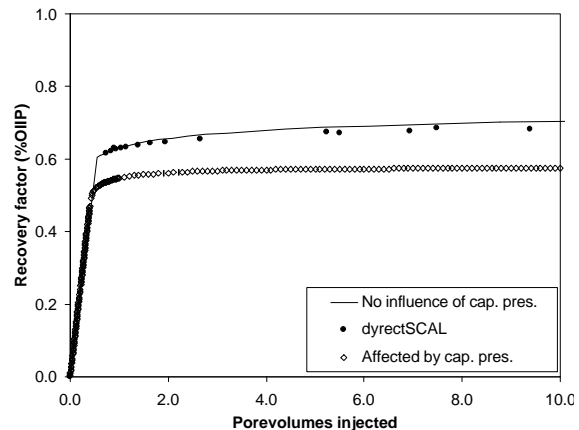


Figure 12 Comparison of interpreted oil recovery factor

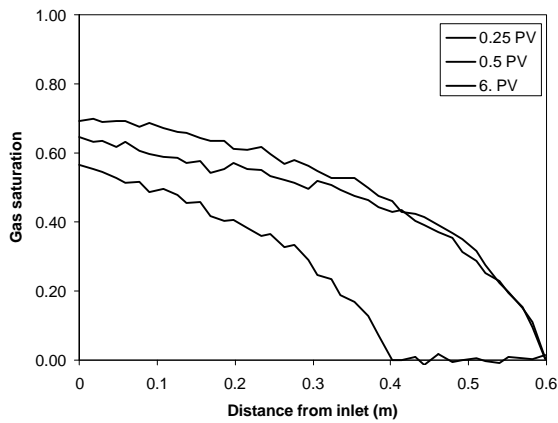


Figure 13 Synthetic gas saturations for gravity drainage test

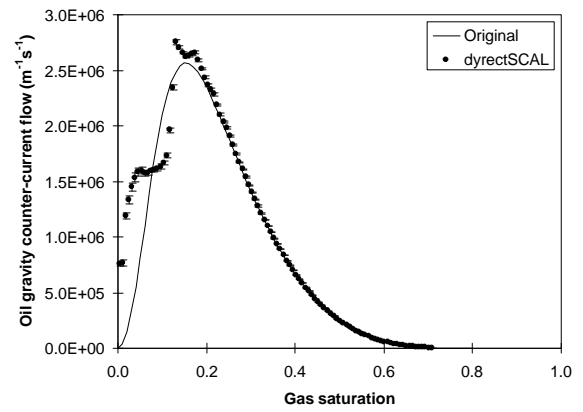


Figure 14 Interpreted counter-current flow velocity for gravity drainage test without noise

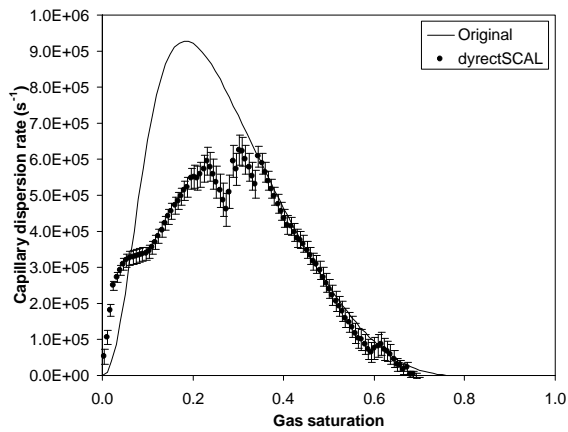


Figure 15 Interpreted capillary dispersion rate for gravity drainage test

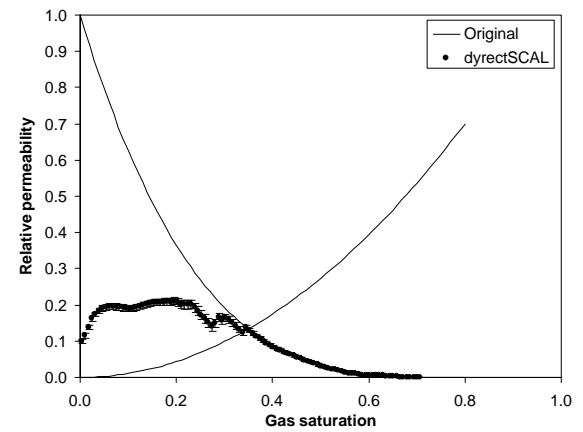


Figure 16 Interpreted oil relative permeability for gravity drainage test

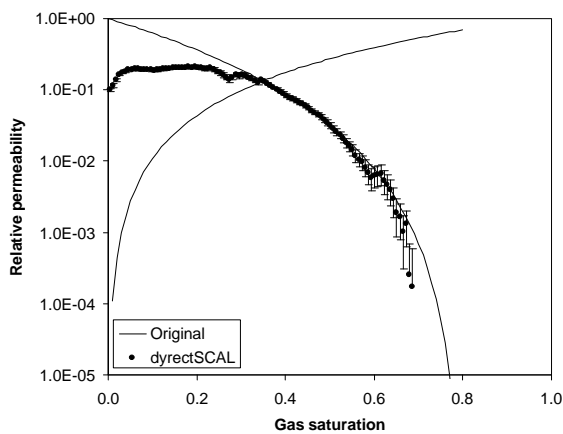


Figure 17 Interpreted oil relative permeability for gravity drainage test

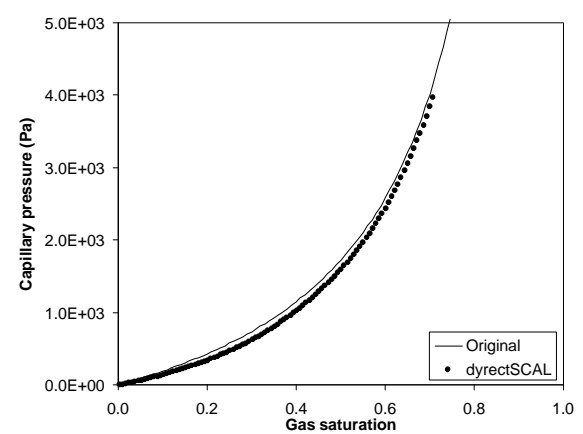


Figure 18 Interpreted gas-oil capillary pressure for gravity drainage test